Polytypism in $LaOBiS_2$-type compounds based on different three-dimensional stacking sequences of two-dimensional BiS_2 layers

Qihang Liu,* Xiuwen Zhang, and Alex Zunger

Renewable and Sustainable Energy Institute (RASEI), University of Colorado, Boulder, Colorado 80309, USA

(Received 14 October 2015; revised manuscript received 12 May 2016; published 31 May 2016)

$LaOBiS_2$-type materials have drawn much attention recently because of various interesting physical properties, such as low-temperature superconductivity, hidden spin polarization, and electrically tunable Dirac cones. However, it was generally assumed that each $LaOBiS_2$-type compound has a unique and specific crystallographic structure (with a space group $P4/nmm$) separated from other phases. Using first-principles total energy and stability calculations we confirm that the previous assignment of the $P4/nmm$ structure to $LaOBiS_2$ is incorrect. Furthermore, we find that the unstable structure is replaced by a *family* of energetically closely spaced modifications (polytypes) differing by the layer sequences and orientations. We find that the local Bi-S distortion leads to three polytypes of $LaOBiS_2$ with different stacking patterns of the distorted BiS_2 layers. The energy difference between the polytypes of $LaOBiS_2$ is merely ~1 meV/u.c., indicating the possible coexistence of all polytypes in the real sample and that the particular distribution of polytypes may be growth induced. The in-plane distortion can be suppressed by pressure, leading to a phase transition from polytypes to the high-symmetry $P4/nmm$ structure with a pressure larger than 2.5 GPa. In addition, different choices of the intermediate atoms (replacing La) or active atoms (BiS_2) could also manifest different ground-state structures. One can thus tune the distortion and the ground state by pressure or by substituting covalence atoms in the $LaOBiS_2$ family.

DOI: 10.1103/PhysRevB.93.174119

I. INTRODUCTION

$LaOBiS_2$ represents a group of materials consisting of BiS_2 layers whose states dominate the low-energy spectrum, separated by electronically passive La_2O_2 buffer layers. $LaOBiS_2$-type materials have drawn attention because of the measured superconductivity [1–14] (up to $T_c = 10.6$ K) and because the BiS_2 layer is spin-orbit active and thus leads to many interesting spin-related properties, including hidden spin polarization [15], spin field-effect transistor [16], and electrically tunable Dirac cones [17]. The general crystal structure consists of a stack of layers $(BiS_2)^-/(La_2O_2)^{2+}/(BiS_2)^-$ made of two BiS_2 rocksaltlike layers and an intermediate fluoritelike La_2O_2 buffer layer separating them [18]. Many materials described by this structural scheme have recently been synthesized [1,2,4,5,7,9,10,14], and even more members not listed in the inorganic crystal structure database (ICSD) can be conceived [17,19]. As with many other compounds, here too it was generally assumed that each compound has a unique and specific crystallographic structure separated from other phases. Using first-principles calculations we find that contrary to this view [1,6,8,11,12,18] the three-dimensional (3D) structure of this important family of compounds represents instead a family of energetically closely spaced modifications differing by the layer sequences and orientations. Such *polytypes* are "natural superlattices," familiar from other areas in condensed matter such as SiC [20,21], ZnX ($X = $ S,Se,Te) [22–24], and $ATiO_3$ ($A = $ Sr and Ba) perovskites [25,26]. Polytypes hold a special place as structural phases in that they have very similar (within meV) total energies, yet are distinguished by those physical properties that are sensitive to orientation and stacking such as polarization of light emission and sometimes the magnitude of the zone-folded band gap (for example, the optical band gap of cubic vs wurtzite polytype of SiC differ by nearly 1 eV [27]). What makes $LaOBiS_2$ polytypes discovered here particularly interesting is that (i) the characteristic local structural distortions in the electronically active BiS_2 layers could lead to charge fluctuations which may be related to the electron-phonon coupling and the mechanism of superconductivity [1,28]; and (ii) different polytypes are either centrosymmetric or noncentrosymmetric, a distinction that carries with it different physical properties related to the presence or absence of inversion symmetry, such as band splitting, second-harmonic generation, and (hidden) spin polarization [15].

In this paper we use first-principles total energy calculations to assess the structure and stability of various polytypes in the $LaOBiS_2$-family of compounds. We find that the local Bi-S distortion leads to three polytypes of $LaOBiS_2$ according to the different stacking pattern of distorted BiS_2 layers, rather than the previously assumed $P4/nmm$ structure. The in-plane distortion is mainly induced by the interaction between the intermediate LaO and the BiS_2 layers, and the electron hybridization in the BiS_2 layer. We performed structural optimization in steps starting from the most restricted degrees of freedom to show how a small distortion can transform the assumed unstable structure to its three polytypes. Since the energy difference between the polytypes of $LaOBiS_2$ is merely ~1 meV/u.c., the real 3D material constructed by stacking up such three types of building blocks could manifest various sequences of polytypes depending sensitively on the growth condition. Furthermore, the in-plane distortion can be suppressed by pressure, leading to a phase transition from polytypes to the high-symmetry $P4/nmm$ structure with a pressure larger than 2.5 GPa. In addition, different choices of the buffer atoms (replacing La) or active atoms (BiS_2) manifest different ground-state polytypes.

*qihang.liu85@gmail.com

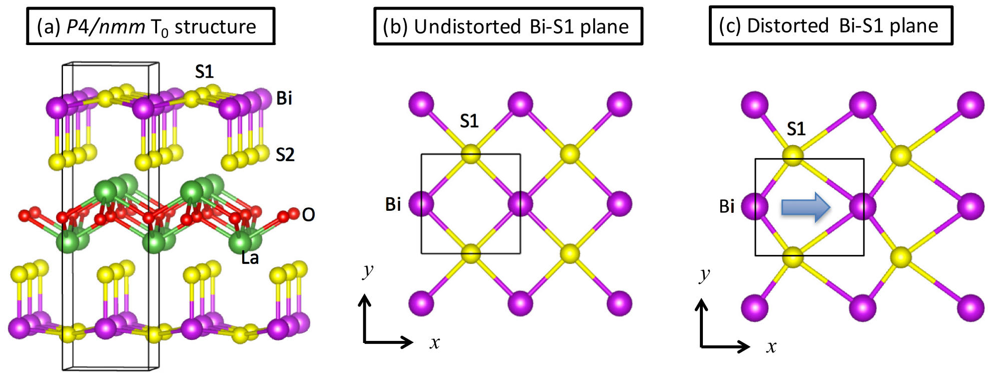

FIG. 1. (a) $P4/nmm$ T_0 structure of $LaOBiS_2$. (b) Top view of Bi-S1 2D square consisting of Bi and S1 atoms in T_0 structure. (c) Top view of Bi-S1 2D square with distortion. The blue arrow along the x direction indicates the displacement of S1 and the spontaneous polarization. The black frame indicates the unit cell.

II. THE IN-PLANE STRUCTURE OF THE TWO-DIMENSIONAL BiS_2-LIKE LAYER AND THE EMERGENCE OF POSSIBLE STACKING SEQUENCES

$LaOBiS_2$ [18] has been generally accepted to have the ZrCuSiAs-type structure, with a centrosymmetric $P4/nmm$ space group. X-ray diffraction data were refined [1,6] by fitting the measured intensities to this structure type (named T_0 hereafter). In T_0 the BiS_2 layers in the $(BiS_2)^-/(La_2O_2)^{2+}/(BiS_2)^-$ stacks have four equal Bi-S bonds, as shown in Fig. 1. However, recent phonon calculations using density functional theory (DFT) found that the T_0 structure with *assumed* equal Bi-S bond lengths of 2.89 Å has soft phonons at the Brillouin zone center Γ point, which indicates dynamic instability and the theoretical impossibility of this T_0 structure [11] being stable. Yildirim showed that by shifting the S atoms along the diagonal of the two-dimensional (2D) square [x or y direction in Fig. 1(b)], forming a ferroelectriclike distortion with two different in-plane Bi-S bonds [bond lengths 2.80 and 2.98 Å; see Fig. 1(c)] one can remove the dynamic instability. In this calculation a deformation parameter Q, which is defined by the normal modes having the unstable phonon, was introduced to represent the in-plane displacement of S atoms. The total energy was minimized with respect to Q, with the remaining structural degrees of freedom other than Q (such as lattice parameter and atomic positions) kept frozen at their $Q = 0$ value (corresponding to the T_0 structure). A subsequent neutron powder diffraction experiment by Athauda *et al.* [29] confirmed this predicted *local* distortion within a single BiS_2 layer by observing indeed two different Bi-S bonds (with lengths of 2.68 and 3.11 Å). We note that the powder diffraction also suggested another antiferroelectriclike distortion [29], but such a mode is predicted to induce an instability at M point that is present in F-doped $LaOBiS_2$ but absent in the parent compound, and was thus excluded by single-crystal diffraction very recently [30].

However, the in-plane *local distortions* predicted [11] and observed [29] do not define as yet a 3D structure in $LaOBiS_2$: There are two BiS_2 layers in a unit cell, and one needs to construct a 3D model of how the various 2D layers are stacked so as to minimize the energy. Yildirim [11] suggested a 3D structure that consists of two BiS_2 layers having the *same direction of distortion* [illustrated by the blue arrow shown in Fig. 1(c)] as a replacement of the unstable T_0 structure. This ferroelectriclike structure removes the phonon instability and thus lowers the energy, turning the 3D structure into noncentrosymmetric T_1 (space group $P2_1mn$) from centrosymmetric T_0 ($P4/nmm$) [11]. Interestingly, there are additional 3D stacking sequences of the 2D layers possible that were not previously examined in pristine $LaOBiS_2$ (without doping) by aligning the in-plane distortion in different directions. There are three possible stacking types that fulfill the local Bi-S1 distortion [11,29]. In the T_1 type, the local distortions of two BiS_2 layers are *along* the x direction, and in T_2 they occur along the x and $-x$ directions, while in T_3 they are along the x and y directions. These distortions lower the system's symmetry from $P4/nmm$ (T_0) to $P2_1mn$ (T_1), or $P2_1/m$ (T_2) or $C2$ (T_3). Among T_1, T_2, and T_3, only T_2 is centrosymmetric, whereas T_1 and T_3 are noncentrosymmetric. We next inquire as to the energetic order of stability of the different polytypes in $LaOBiS_2$ as well as in other compounds from the same general family.

III. METHODS OF CALCULATION

The geometrical and electronic structures are calculated by the projector-augmented wave (PAW) pseudopotential [31] and the generalized gradient approximation of Perdew, Burke, and Ernzerhof (PBE) [32] to the exchange-correlation functional as implemented in the Vienna *ab initio* package (VASP) [33]. The plane-wave energy cutoff is set to 550 eV. Electronic energy minimization was performed with a tolerance of 10^{-6} eV, and all atomic positions were relaxed with a tolerance of 10^{-3} eV/Å.

We note that the PBE functional does not take the long-range van der Waals interaction into account, and thus usually overestimates the interlayer space. To overcome this, we also use the PBE-D2 exchange-correlation functional, with the implementation of the van der Waals (VDW) correction, to optimize the distorted structures (see Sec. VI).

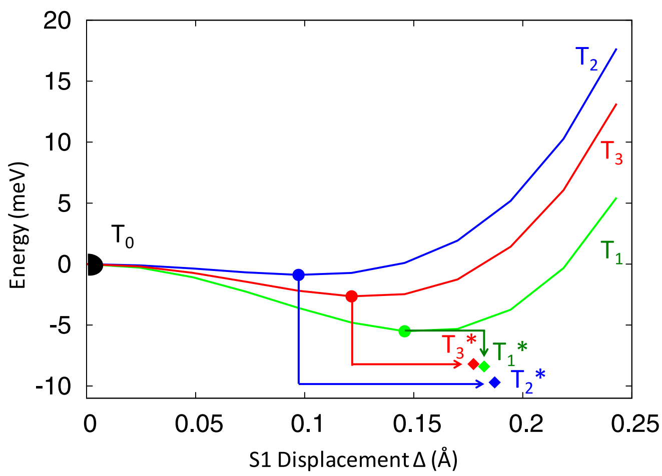

FIG. 2. Total energy as a function of S1 displacement in $T_1 - T_3$ stacking types of $LaOBiS_2$. $T_1^* - T_3^*$ indicate the complete relaxed structures of $T_1 - T_3$ type [approach (c)], respectively.

IV. THREE LEVELS OF APPROXIMATION FOR PREDICTING BOND RELAXATION AND SYMMETRY BREAKING

The three polytypes differ in the stacking direction of electronic-active BiS_2 layers along the [001] direction. To gain insight into the various degrees of freedom we perform structural optimization in steps starting from the simplest and most restricted:

Approach (a). If one allows the T_0 structure to relax but without imposing initially any symmetry breaking, only the a, c lattice vectors and four independent cell-internal atomic coordinate parameters (atomic positions of La, Bi, S1, and S2 sites along the c axis) can relax. This restricted relaxation is an artifact of the method of calculation, namely, of assuming initially a high-symmetry structure. It reflects the fact that the other degrees of freedom in T_0 that could relax are not permitted to do so because a high symmetry (zero force on atoms) is artificially imposed. As a result, the final structure in this relaxation method still has the same space group $P4/nmm$ as the initial starting point, denoted by the T_0 point in Fig. 2. Although this is the only optimization treatment in most structure determination steps in the DFT community, the result is incorrect because of the artificial restriction to high symmetry.

Approach (b). Next, we allow in-plane relaxation by initially lowering the symmetry but freeing all other degrees of freedom, while seeking the energy minimum under this constrain. To do so we start from T_0 but shift the S1 atom of each BiS_2 layer along the x or y direction (depending on the $T_1 - T_3$ type) and artificially *keep all other structural degrees of freedom frozen.* Such frozen Bi-S1 "bond length mismatch" distortion has been used in Ref. [11] for T_1 and is defined by the S1 displacement Δ. This is not the most general procedure, and it is used here to observe what its physical consequence is. This simplified procedure of allowing just one mode to drive distortion is common in simple models of phase transitions. The results of this simplified model are the three curves in Fig. 2. They show that if one scans the energy as a function of Δ, each of these structures has different energy minima shown as solid dots in the $T_1 - T_3$ curves. ***This is clear evidence that in $LaOBiS_2$ the T_0 structure is a saddle point and thus is not able to exist stably.***

Approach (c) (most general). The in-plane Bi-S1 distortion can enable additional degrees of freedom, including the lattice parameters and atomic positions. For example, T_1-type distortion will elongate the axis, while T_2-type distortion will twist the rectangular $x - z$ plane of the unit cell into a parallelogram. Therefore, in the most general approach (c) we further relax all degrees of freedom starting from the energy-minimum structures of $T_1 - T_3$, and get three final structures that are several meV/unit cell (u.c.) lower in energy, T_1^*, T_2^*, and T_3^* indicated in Fig. 2 by diamond shapes. Unlike the T_0 structure, the T_1^*, T_2^*, and T_3^* structures are thermodynamically stable. We also considered full relaxation starting from a generic symmetry breaking of the T_0 structure by randomly adding small distortions on both lattice vectors and atomic positions. We find from a few such starting points that the relaxed structures all become T_1^*, T_2^*, or T_3^* structure, indicating that $T_1^* - T_3^*$ structures are the only three local minima around the T_0 phase.

Comparison between different fully relaxed polytypes. Table I shows the total energy, space group, lattice parameter, and Bi-S bond length of T_0, $T_1^* - T_3^*$ structure as well as the experimental refinement using T_0 structure. Several observations are found: (i) Although the T_0 structure has a good agreement and a reasonable fit [6]

TABLE I. The stacking configurations of in-plane distortion, space group, inversion symmetry, total energy per u.c., Bi-S bond lengths, and lattice parameters of $LaOBiS_2$, including experimental results and DFT calculations T_0 and $T_1^* - T_3^*$ on the PBE level. The total energy of the T_0 structure is set to zero as a reference.

	Experiment [29]	T_0	T_1^*	T_2^*	T_3^*
Stacking of distortion		No distortion	(x,x)	$(x,-x)$	(x,y)
Space group	$P4/nmm$	$P4/nmm$	$P2_1mn$	$P2_1/m$	$C2$
Inversion symmetry	Unknown	Yes	No	Yes	No
Energy (meV)		0	–8.4	–9.7	–8.2
Bi-S bond (Å)	2.68/ 3.11	2.89/ 2.89	2.77/ 3.03	2.76/ 3.04	2.77/ 3.03
a (Å)	4.054	4.050	4.071	4.073	4.060
b (Å)	4.054	4.050	4.051	4.051	4.060
c (Å)	13.825	14.250	14.266	14.273	14.266

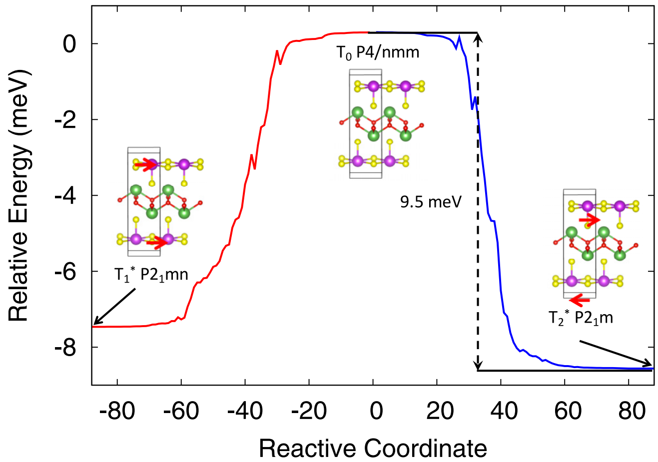

FIG. 3. Total energy change during the transformation from T_1^* to T_2^* structure with T_0 structure as an intermediate state. The reaction coordinate in the x axis is presented by the DFT relaxation steps from T_0 to T_1^* and T_2^*. The red and blue lines denote the transition from T_0 to T_1^* and T_2^*, respectively. The red arrows in the crystal structure denote the direction of the BiS_2 in-plane distortion.

(R factor <0.1) with experiment regarding the in-plane lattice constant, there is only one kind of Bi-S bond, which is inconsistent with the results by neutron diffraction [29]. On the other hand, all of T_1^* to T_3^* suggests two kinds of in-plane Bi-S1 bonds, with the bond lengths 2.76–2.77 and 3.03–3.04 Å, respectively. These bond lengths agree well with the experiments [29]. (ii) With the presence of the in-plane distortion for $T_1^* - T_3^*$ structures relative to T_0, the buckling nature of the Bi-S1 plane is nearly unchanged. The calculated S1-Bi-S1 angle varies from 165° for T_0 to 164° for all $T_1^* - T_3^*$ structures, including one type of S1-Bi-S1 angle in T_1^* and T_2^*, and two types in T_3^*. (iii) The T_2^* structure is centrosymmetric and has the lowest energy, but is only 1–2 meV/u.c. lower than the noncentrosymmetric T_1^* and T_3^*. Such a small energy difference originates from the weak van der Waals interaction between adjacent BiS_2 layers. The total energies of the polytypes are so close that theoretical stability could be significantly affected by the temperature or crystal growing conditions. On the other hand, T_0 structure has the highest energy, about 10 meV/u.c. higher than T_2^*.

In order to visualize the transformation path from the saddle point T_0 to the stable structures (e.g., T_1^* or T_2^*) in $LaOBiS_2$, we show in Fig. 3 the feasibility of converting $LaOBiS_2$ from T_1^* to T_2^* structure with T_0 structure as an intermediate state. In the $T_0 \rightarrow T_1^*$ and $T_0 \rightarrow T_2^*$ paths we start from T_0 structure and impose a tiny T_1- or T_2- type distortion on T_0. Then we record each step of the DFT relaxation process from T_0 to T_1^* (T_2^*) as the reaction coordinate, i.e., the geometric parameter that changes during the conversion between T_1^* and T_2^*, by gradually changing the cell and the atomic position using the conjugate gradient method. We find that T_0 structure stays at a saddle point, so it is unstable and will spontaneously relax to a distorted structure T_1^* or T_2^* (also probably T_3^*). On the other hand, the potential barrier between the transition of T_1^* and T_2^* structures is about 10 meV, which is not large enough to make T_2^* as a unique structure. Instead, it is possible for all T_1^* to T_3^* structures or their mixed phases to happen at room temperature.

V. PRESSURE-INDUCED PHASE TRANSITION AND POLYTYPES IN OTHER $LaOBiS_2$-TYPE COMPOUNDS

In order to unveil the physical origin of the polytypism, we investigated the ground-state structure of $LaOBiS_2$ under hydrostatic pressure. Figure 4(a) shows the in-plane distortion of $T_1 - T_3$ structures presented by the Bi-S1 bond difference as a function of hydrostatic pressure. Zero pressure $P = 0$ corresponds to $T_1^* - T_3^*$ structures with a PBE-calculated equilibrium lattice constant. We find that the pressure indeed suppresses the in-plane distortion for all $T_1 - T_3$ structures. Above $P = 2.5$ GPa (corresponding to an in-plane lattice constant $a = b = 4.02$ Å) the high-symmetry T_0 structure becomes the ground state of $LaOBiS_2$.

Following $LaOBiS_2$, many compounds having similar structure are reported for the purpose of exploring the BiS_2-based superconductivity [7,10]. Therefore, it is interesting to ask if the other compounds in this family also have such polytypes or not, and what determines T_0 structure or distorted structures as a ground state. We substitute La (with Y), Bi (with Sb, As) or S (with Se, Te) site at one time and fix the other three sites the same as $LaOBiS_2$. Figure 4(b) shows the relative energy of the polytypes of these materials. We found that when substituting La with lighter elements or substituting S with heavier elements, the undistorted T_0 structures are the ground states, which means there are no polytypes in these materials. On the other hand, when substituting Bi with lighter elements Sb and As, T_0 structures are no longer dynamic stable (dash lines), while distorted $T_1^* - T_3^*$ are local minima. Among them T_2^* is the ground state, with the total energy 10–15 meV lower than that of T_1^*. The energy differences between T_2^* and T_0 for $LaOSbS_2$ and $LaOAsS_2$ are 167 and 718 meV, respectively, which is much larger than the counterpart of $LaOBiS_2$. Moreover, the in-plane M-S1 bonds (M: Bi, Sb, or As) also reveal that $LaOSbS_2$ and $LaOAsS_2$ suffer larger distortion. The two As-S1 bond lengths in $LaOAsS_2$ are 2.43 and 3.31 Å. As a result, such large distortion breaks the 2D As-S square and forms individual zigzag As-S chains, as shown in the inset of Fig. 4(b).

From the study of pressure and various $LaOBiS_2$-type compounds we conclude that the polytypism in the $LaOBiS_2$ family is mainly attributed to two reasons: the "substrate" effect of the intermediate layer (e.g., LaO) and the hybridization effect of the active layer (e.g., BiS_2). In $LaOMS_2$ compounds (M: Bi, Sb, As), the mismatch between the optimum lattice constants of LaO (larger) and MS_2 (smaller) layers tends to stretch the M-S square and thus cause distortion. When the lattice of MS_2 layers becomes smaller without changing the LaO layer, the stretching effect becomes stronger. Interestingly, although this effect originates from the interaction between LaO and MS_2 layers, the distortion in the LaO layer is insignificant. It is because the bond energy of La-O is large so that the LaO network remains stable when suffering distortions. On the other hand, enlarging the lattice parameter of the side layer or reducing the lattice parameter of the intermediate layer induces better lattice match between the side and intermediate layers so that the distortion is unlikely to happen, as in the

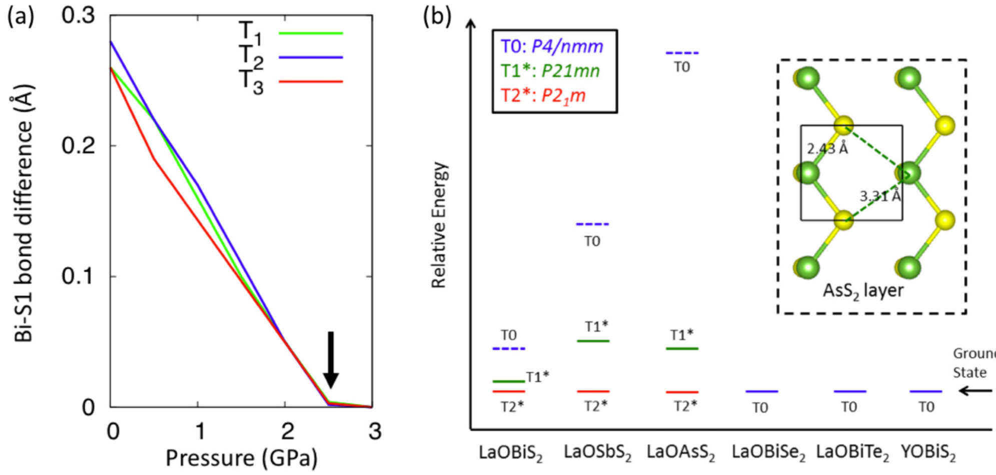

FIG. 4. (a) The difference of bond length within Bi-S1 plane of distorted $T_1 - T_3$ structures as a function of hydrostatic pressure. The black arrow corresponds to 2.5 GPa where the Bi-S1 bond length becomes isotropic, indicating a phase transition from a distorted structure to a high-symmetry T_0 structure. Since the difference between a distorted $T_1 - T_3$ and T_0 structure is just a stretched Bi-S1 plane (but no bond breaking), different pressure will lead to a structure with either larger or smaller in-plane distortion. If the distortion vanishes under pressure, then a phase transition will ensue from $T_1 - T_3$ to T_0. (b) Schematic illustration of the relative energy of different polytypes in the $LaOBiS_2$ family. The dashed horizontal lines denote structures that are dynamic unstable. Dashed box: top view of AsS_2 layer in $LaOAsS_2$, in which the unit cell is denoted by the solid frame. The strong distortion separates the layer into individual zigzag chains.

case in $LaOBiSe_2$,$LaOBiTe_2$, and $YOBiS_2$. For $LaOBiS_2$ under pressure, the BiS_2 and LaO layers are simultaneously compressed, in which case the enhanced Bi-S1 bond strength could stabilize the T_0 structure and prevent distortion.

The other factor that can lead to distortion is the composition of the side layer. For the trend from Bi to As, the group V cations behave with more covalent character and less ionic character. As a result, they are inclined to form sp^3 hybridization with three S atoms and the other bond is the lone-pair electron. The lone-pair bond usually has a larger repulsive force than the other bonds, and thus breaks two M-S1 bonds to form zigzag chains.

VI. THE RESULTS OF VDW CORRECTION

VDW interactions represent the interaction of an *induced moment* (dipole, quadropole, etc.) with itself. This is strictly zero in mean field Hartree-Fock or DFT. From Table I we find that DFT without VDW gives the length of the c axis (T_0 and $T_1^* - T_3^*$) as 14.25 Å, much larger than the observed 13.83 Å. This is because the PBE functional does not take the long-range van der Waals interaction into account, and thus usually overestimates the interlayer space.

To overcome this, we also use PBE-D2 exchange-correlation functional that includes a rough VDW term to optimize the distorted structures. We find that the a and c axes of the T_0 structure are 3.99 and 13.62 Å, respectively. Although PBE-D2 gives better agreement with experiments on the c axis (13.83 Å), it underestimates the a axis by 1.5% compared to experiments or PBE results (4.05 Å). More importantly, because of the biaxial strain effect within the x-y plane under the PBE-D2 method, the undistorted structure T_0 becomes the ground state. We performed the relaxation starting from the PBE relaxed T_1^*-T_3^* structure and find that the final configuration is the T_0 structure. Phonon calculations of $LaOBiS_2$ for smaller in-plane lattice parameters also suggested that the undistorted structure T_0 is dynamic stable [11]. Since the accuracy of the a axis is more important for investigating the in-plane distortion, we used the PBE functional for the base of our calculation and analysis.

VII. SUMMARY

By using first-principles total energy and stability calculations, we predict that the local Bi-S distortion leads to three polytypes of $LaOBiS_2$-type materials according to the different stacking pattern of BiS_2-like layers. The in-plane distortion, mainly induced by the interaction between the intermediate and the side layers and the electron hybridization in the side layer, can lower the total energy compared with the conventionally accepted $P4/nmm$ structure. In $LaOBiS_2$, the energy difference between the polytypes is small, indicating the possible coexistence of all polytypes in the real sample. While we cannot determine if the superposition is dynamic in nature (time-dependent doping); we note that such a superstructure with the combination of T_1,T_2, and T_3 polytypes will effectively lower the symmetry to the P1 space group. Such a superstructure symmetry has been recently suggested by a single-crystal neutron-diffraction experiment of Athauda *et al.* [30]. Finally, external pressure and different choices of the intermediate atoms (replacing La) or active atoms (BiS_2) manifest different ground-state polytypes. One can thus tune the distortion and the ground state by both physical and chemical means. Our findings provide a clear picture on the complexity of the crystal structure of $LaOBiS_2$-type materials, which might be relevant to the mechanism of the recently found BiS_2-based superconductivity.

ACKNOWLEDGMENTS

We are grateful for the helpful discussions with Professor Daniel Dessau from University of Colorado Boulder and Professor Despina Louca from University of Virginia. This work was supported by the National Science Foundation (NSF) grant titled "Theory-Guided Experimental Search of Designed Topological Insulators and Band-Inverted Insulators" (Grant No. DMREF-13-34170). This work used the Extreme Science and Engineering Discovery Environment (XSEDE), which is supported by NSF Grant No. ACI-1053575.

[1] Y. Mizuguchi, S. Demura, K. Deguchi, Y. Takano, H. Fujihisa, Y. Gotoh, H. Izawa, and O. Miura, J. Phys. Soc. Jpn. **81**, 114725 (2012).
[2] S. K. Singh, A. Kumar, B. Gahtori, Shruti, G. Sharma, S. Patnaik, and V. P. S. Awana, J. Am. Chem. Soc. **134**, 16504 (2012).
[3] H. Usui, K. Suzuki, and K. Kuroki, Phys. Rev. B **86**, 220501 (2012).
[4] J. Xing, S. Li, X. Ding, H. Yang, and H.-H. Wen, Phys. Rev. B **86**, 214518 (2012).
[5] S. Demura, Y. Mizuguchi, K. Deguchi, H. Okazaki, H. Hara, T. Watanabe, S. J. Denholme, M. Fujioka, T. Ozaki, H. Fujihisa, Y. Gotoh, O. Miura, T. Yamaguchi, H. Takeya, and Y. Takano, J. Phys. Soc. Jpn. **82**, 033708 (2013).
[6] J. Lee, M. B. Stone, A. Huq, T. Yildirim, G. Ehlers, Y. Mizuguchi, O. Miura, Y. Takano, K. Deguchi, S. Demura, and S. H. Lee, Phys. Rev. B **87**, 205134 (2013).
[7] H. Lei, K. Wang, M. Abeykoon, E. S. Bozin, and C. Petrovic, Inorg. Chem. **52**, 10685 (2013).
[8] B. Li, Z. W. Xing, and G. Q. Huang, Europhys. Lett. **101**, 47002 (2013).
[9] X. Lin, X. Ni, B. Chen, X. Xu, X. Yang, J. Dai, Y. Li, X. Yang, Y. Luo, Q. Tao, G. Cao, and Z. Xu, Phys. Rev. B **87**, 020504 (2013).
[10] W. A. Phelan, D. C. Wallace, K. E. Arpino, J. R. Neilson, K. J. Livi, C. R. Seabourne, A. J. Scott, and T. M. McQueen, J. Am. Chem. Soc. **135**, 5372 (2013).
[11] T. Yildirim, Phys. Rev. B **87**, 020506 (2013).
[12] A. Athauda, J. Yang, B. Li, Y. Mizuguchi, S. Lee, and D. Louca, J. Supercond. Novel Magn. **28**, 1255 (2015).
[13] K. Terashima, J. Sonoyama, T. Wakita, M. Sunagawa, K. Ono, H. Kumigashira, T. Muro, M. Nagao, S. Watauchi, I. Tanaka, H. Okazaki, Y. Takano, O. Miura, Y. Mizuguchi, H. Usui, K. Suzuki, K. Kuroki, Y. Muraoka, and T. Yokoya, Phys. Rev. B **90**, 220512 (2014).
[14] H.-F. Zhai, P. Zhang, S.-Q. Wu, C.-Y. He, Z.-T. Tang, H. Jiang, Y.-L. Sun, J.-K. Bao, I. Nowik, I. Felner, Y.-W. Zeng, Y.-K. Li, X.-F. Xu, Q. Tao, Z.-A. Xu, and G.-H. Cao, J. Am. Chem. Soc. **136**, 15386 (2014).
[15] X. Zhang, Q. Liu, J.-W. Luo, A. J. Freeman, and A. Zunger, Nat. Phys. **10**, 387 (2014).
[16] Q. Liu, Y. Guo, and A. J. Freeman, Nano Lett. **13**, 5264 (2013).
[17] X.-Y. Dong, J.-F. W., R.-X. Zhang, W.-H. Duan, B.-F. Zhu, J. Sofo, and C.-X. Liu, Nat. Commun. **6**, 8517 (2015).
[18] V. S. Tanryverdiev, O. M. Aliev, and I. I. Aliev, Inorg. Mater. **31**, 1361 (1995).
[19] Q. Liu, X. Zhang, H. Jin, K. Lam, J. Im, A. J. Freeman, and A. Zunger, Phys. Rev. B **91**, 235204 (2015).
[20] C. Cheng, R. J. Needs, and V. Heine, J. Phys. C: Solid State Phys. **21**, 1049 (1988).
[21] A. Qteish, V. Heine, and R. J. Needs, Phys. Rev. B **45**, 6534 (1992).
[22] Y. Hao, G. Meng, Z. L. Wang, C. Ye, and L. Zhang, Nano Lett. **6**, 1650 (2006).
[23] M. I. B. Utama, M. de la Mata, C. Magen, J. Arbiol, and Q. Xiong, Adv. Funct. Mater. **23**, 1636 (2013).
[24] F. Boutaiba, A. Belabbes, M. Ferhat, and F. Bechstedt, Phys. Rev. B **89**, 245308 (2014).
[25] W. Zhong and D. Vanderbilt, Phys. Rev. Lett. **74**, 2587 (1995).
[26] W. Zhong and D. Vanderbilt, Phys. Rev. B **53**, 5047 (1996).
[27] C.-Y. Yeh, S.-H. Wei, and A. Zunger, Phys. Rev. B **50**, 2715 (1994).
[28] X. Wan, H.-C. Ding, S. Y. Savrasov, and C.-G. Duan, Phys. Rev. B **87**, 115124 (2013).
[29] A. Athauda, J. Yang, S. Lee, Y. Mizuguchi, K. Deguchi, Y. Takano, O. Miura, and D. Louca, Phys. Rev. B **91**, 144112 (2015).
[30] A. Athauda, C. Hoffman, Y. Ren, S. Aswartham, J. Terzic, G. Cao, X. Zhu, and D. Louca, arXiv:1601.07517 (2016).
[31] G. Kresse and D. Joubert, Phys. Rev. B **59**, 1758 (1999).
[32] J. P. Perdew, K. Burke, and M. Ernzerhof, Phys. Rev. Lett. **77**, 3865 (1996).
[33] G. Kresse and J. Furthmüller, Comput. Mater. Sci. **6**, 15 (1996).